

Classification of Oppenheimer-Snyder Collapse: Singular, Bouncing, and Soft-Landing Scenarios

Zhi-Chao Li ¹, H. Khodabakhshi ¹ and H. Lü ^{1,2}

¹*Center for Joint Quantum Studies, Department of Physics,
School of Science, Tianjin University, Tianjin 300350, China*

²*The International Joint Institute of Tianjin University, Fuzhou,
Tianjin University, Tianjin 300350, China*

Abstract

We study Oppenheimer-Snyder (OS) gravitational collapse matched to a general static, spherically symmetric exterior spacetime. Unlike the Schwarzschild case, two new features can arise in black holes with two horizons: an *apparent-horizon left vertex*, a temporary minimum in the apparent-horizon radius during collapse, and a *bounce*, where the star surface stops collapsing at a nonzero radius and reverses into expansion. We identify the conditions that lead to these two features. For two-horizon exteriors, trapped-region consistency requires that the apparent-horizon turning point occurs no earlier than the surface crossing of the inner horizon. As a concrete example, the OS collapse of the Reissner-Nordström (RN) spacetime shows both effects. In contrast, regular black holes with de Sitter cores show neither: their collapse is smooth and monotonic, and the surface approaches the center only as the proper time goes to infinity. These results naturally classify the OS collapses into three categories: *singular*, which ends at the center in finite time; *bouncing*, which reverses at a finite radius; and *soft-landing*, which reaches the center only asymptotically. We argue that these features are consistent with Penrose's strong cosmic censorship conjecture.

Contents

1	Introduction	3
2	OS collapse dynamics	5
3	Bounce and apparent-horizon vertex	6
3.1	Apparent-horizon vertex	7
3.2	Star-surface bounce	7
3.3	Interplay between the bounce and the left vertex	9
4	RN collapse: a bounce with a vertex	9
4.1	Apparent-horizon vertex	10
4.2	Star-surface bounce	11
5	Regular black hole collapse	14
5.1	Regular black holes: no bounce or vertex	14
5.2	Regular core-based classification	15
6	Conclusion	16
Appendix A OS collapse of regular EMS black holes		18
Appendix B OS collapse of critical Born-Infeld black hole		19

1 Introduction

Gravitational collapse is one of the most important predictions of General Relativity and provides the theoretical foundation for black hole formation. The classic OS model [1] describes how a homogeneous, pressureless dust star collapses into a Schwarzschild black hole. This is achieved by smoothly matching an interior Friedmann-Lemaître-Robertson-Walker (FLRW) spacetime to a vacuum exterior (Schwarzschild metric) using the Israel junction conditions [2]. In this idealized picture, the star surface reaches the central spacelike singularity in finite proper time, while trapped surfaces and apparent horizons form, and the star continues to shrink and eventually the apparent horizon aligns with the star surface as it collapses to zero size.

There are additional black holes beyond the Schwarzschild black hole. A notable example is the RN black hole. It is thus of interest to study generalized OS collapse such that the exterior of the collapsing star surface is described by a general spherically-symmetric black hole metric, namely

$$ds^2 = -h(r)dt^2 + \frac{dr^2}{f(r)} + r^2d\Omega_2^2. \quad (1)$$

However, it turns out that the consistency conditions on the matching between the interior FLRW spacetime and the exterior static metric (1) require that $h = f$ [3]. In other words, the generalized OS collapse beyond the Schwarzschild black hole applies only to the special static metric with $g_{tt}g_{rr} = -1$. Nevertheless, there still exist large classes of static black holes that are of the special static type, including the RN black holes and most of the regular black holes, e.g. [4, 5]. In our recent work [6], we generalized OS collapse to an arbitrary special static and spherically-symmetric exterior. We derived general formulae for the surface evolution, as well as for both the apparent and event horizons. We also identified an upper bound on the event-horizon formation time and conjectured that Schwarzschild collapse saturates this bound for fixed mass. We later proved this conjecture in [3], assuming that the matter satisfies the weak energy condition.

Both RN and regular black holes are characterized by having two horizons, the outer event horizon and inner Cauchy horizon. Extending the OS framework to such exteriors can reveal new features. We can illustrate these, using the RN black hole as a concrete example. It turns out that the repulsive effect in the region further inside the inner horizon can stop the collapse at a nonzero radius [6]. Consequently, as we shall demonstrate in this paper, it can produce a *bounce* of the collapsing star surface. Moreover, the apparent horizon needs not evolve monotonically; it can have a local minimum in its trajectory in some parameter region of the mass and charges. We refer to this feature as a *left vertex*.

In this paper, we focus on identifying additional physically meaningful signatures in OS collapse dynamics by considering the more general non-Schwarzschild exterior metric function $f(r)$. In particular, we reveal two independent features that could arise: (i) a *bounce*, where the star’s surface reaches a nonzero finite radius and reverses from collapse to expansion; and (ii) a *left vertex*, where the apparent-horizon radius reaches a temporary minimum during the collapse. A spacetime may exhibit one, both, or neither features. For a physically consistent formation of a two-horizon black hole, the apparent-horizon turning point must occur no earlier than the surface crossing over the inner horizon, so that the relevant apparent-horizon branch connects monotonically between the outer horizon R_+ and the inner horizon R_- [6]. This condition provides a strong constraint on the black hole parameters. In the RN case, it implies a lower bound on the charge, namely $|q| \geq \sqrt{3}m/2$. Importantly, this also ensures that the bounce radius R_* is not negligible, making the bounce a physically meaningful feature. In addition, we introduce a third characteristic scale, namely the *inflection radius* R_{infl} , where the surface acceleration vanishes ($\ddot{R} = 0$) while the collapse is still ongoing. This radius marks the transition from the accelerating phase to the decelerating phase of the collapse, and complements the dynamical picture.

The RN solution provides a clean analytical example in which both signatures are present. In contrast, we show that regular black holes may exhibit neither, despite also having two horizons. In those cases the collapse is smooth and monotonic, and the surface approaches the center only asymptotically in proper time. We shall thus study the local and global criteria for these new features and their physical implications. Our work is also motivated by a desire to better understand black hole interiors, especially about the fate of the inner horizon, associated with the Penrose’s strong cosmic censorship conjecture (SCCC) [7–9]. By identifying simple, geometry-based signatures in the OS framework, we offer a practical way to classify collapse outcomes into three distinct types: *singular* collapse that ends at the center in finite proper time, *bouncing* collapse that reverses at a finite radius, and *soft-landing* collapse that approaches the center only asymptotically. In particular, the bouncing phenomenon indicates the instability of the inner horizon, consistent with the SCCC. We also emphasize that the collapse type can be understood from the joint behavior of the evolutions of the star’s surface $R(T)$ and the apparent horizon $R_{\text{AH}}(T)$, which are physically linked via the proper time T in the OS setup.

The paper is organized as follows. Section 2 reviews the generalized OS collapse dynamics and presents the evolution equations for the star surface and horizons. Section 3 introduces the bounce and left-vertex effects, explains how they lead to a simple classification of exterior spacetimes, and provides the conditions on the exterior metric that give rise to these features,

using the Misner-Sharp mass function [10]. Section 4 applies this framework to the RN case, where both signatures are present. Section 5 extends the analysis to regular black holes, offering a core-based classification of when vertices or bounces can occur and demonstrating that de Sitter-core solutions exhibit neither feature. We conclude in Section 6. We include some further material in Appendices. Appendix A examines electrically-charged regular black holes in Einstein-Maxwell-scalar (EMS) gravity [11]. We show why neither signature appears on the de Sitter-core branch. Appendix B further discusses the critical Born-Infeld exterior as an additional example with neither feature.

2 OS collapse dynamics

In the generalized OS framework [6], a collapsing spherical star is modeled as a homogeneous ball of pressureless dust, described by a FLRW spacetime in its interior. We consider the OS collapse with spatially-flat FLRW interior ($k = 0$), for which the interior geometry admits a convenient Painlevé-Gullstrand (PG)-type slicing. The star is matched at its surface to a special class of static, spherically symmetric exterior geometries of the form

$$ds^2 = -f(r) dt^2 + \frac{dr^2}{f(r)} + r^2 d\Omega^2. \quad (2)$$

By “special class”, we mean that $h = f$ in the general static metric (1). To avoid coordinate singularities on horizons and to work in a time slicing adapted to freely falling observers, we employ PG coordinates, where the interior FLRW metric can be written as

$$ds^2 = -d\tau^2 + (dr - rH(\tau) d\tau)^2 + r^2 d\Omega^2. \quad (3)$$

In the above equation, τ is the proper time of comoving dust particles and $H(\tau) = \dot{a}/a$ is the Hubble parameter (dot denotes $d/d\tau$). On the star surface, the physical radius is $R(\tau) = a(\tau) r_0$, where r_0 is a fixed comoving coordinate. In PG coordinates, the exterior becomes

$$ds^2 = -dT^2 + (dr + \sqrt{1 - f(r)} dT)^2 + r^2 d\Omega^2, \quad (4)$$

where T is the PG time. Along the star surface, the interior proper time τ and the exterior PG time T are identified, so we use a single time parameter T throughout.

Imposing the Israel junction conditions (continuity of the induced metric and extrinsic curvature, with no thin shell) for a dust interior matched to (4) yields the surface evolution equation

$$\dot{R} = \pm \sqrt{1 - f(R)}, \quad H \equiv \frac{\dot{R}}{R} = \pm \frac{\sqrt{1 - f(R)}}{R}, \quad (5)$$

where an overdot denotes d/dT and we take the collapsing star surface ($\dot{R} < 0$). Integrating (5) gives the star's surface evolution as

$$T(R) = - \int_{R_0}^R \frac{d\tilde{R}}{\sqrt{1 - f(\tilde{R})}}. \quad (6)$$

For the Schwarzschild exterior, corresponding to $f(r) = 1 - 2m/r$, the above integration can be easily performed, and an analytic expression can be obtained. Reversing the function $T(R)$, we obtain the star-surface radius $R(T)$ as a function of its proper time T . However, for general $f(r)$, an analytic function $R(T)$ may not exist, and (6) implies that it is more convenient to use the collapsing star-surface radius R as parameter to describe the dynamical collapse evolution. Using R as if it were “time” is certainly allowed since $T(R)$ is a monotonically decreasing function.

During collapse, the boundary of the trapped region inside the star is marked by the *apparent horizon*. In the homogeneous dust interior with $k = 0$, the apparent-horizon radius is $R_{\text{AH}} = 1/|H|$ [6]. Using $H = -\sqrt{1 - f(R)}/R$ from (5), this becomes a function of the instantaneous star-surface radius R , i.e.

$$R_{\text{AH}}(R) = \frac{R}{\sqrt{1 - f(R)}}. \quad (7)$$

We denote by R_+ the outer horizon radius, i.e., the largest positive root of $f(r) = 0$. Since $f(R_+) = 0$, it follows that $R_{\text{AH}}(R_+) = R_+$; thus, at the instant when the surface crosses the outer horizon, the apparent-horizon radius equals the star's surface radius. If there is an inner horizon, the same relation holds at the inner horizon, where $R_{\text{AH}}(R_-) = R_-$. The event horizon can be obtained by backward tracing of outgoing null rays as in Ref. [6].

Together, Eqs. (6) and (7) characterize both the proper time T and apparent-horizon radius R_{AH} as functions of the star-surface radius R . These functions are completely determined by the exterior metric function $f(r)$. In the following sections, we use these expressions to reveal additional physically interesting signatures, namely bounce and vertex, that can arise in the more general non-Schwarzschild exteriors that have two horizons.

3 Bounce and apparent-horizon vertex

In this section we derive local, geometry-based criteria for the two possible signatures that could arise in generalized OS collapse: (i) a left vertex of the apparent-horizon trajectory and (ii) a star-surface bounce. Both criteria can be determined directly from the exterior metric function $f(r)$.

3.1 Apparent-horizon vertex

As the star collapses, the evolution of both the surface radius R and the apparent-horizon radius R_{AH} can be expressed in terms of the time T . However, as mentioned under (6), T is not the most convenient parameter for describing the evolution. Along the star's surface evolution, the apparent horizon is also naturally represented as the parametric curve $(R_{\text{AH}}(R), T(R))$, where R denotes the instantaneous star-surface radius. The time derivative of the apparent horizon becomes

$$\frac{dR_{\text{AH}}}{dT} = \frac{dR_{\text{AH}}}{dR} \dot{R}. \quad (8)$$

Using Eq. (5) on the collapsing branch ($\dot{R} < 0$) and differentiating Eq. (7), we find

$$\frac{dR_{\text{AH}}}{dT} = -\frac{G(R)}{2(1-f(R))}, \quad G(R) \equiv Rf'(R) + 2(1-f(R)). \quad (9)$$

Along the physically allowed surface evolution one has $1-f(R) \geq 0$, so the sign of dR_{AH}/dT is governed by $G(R)$. The trajectory $R_{\text{AH}}(T)$ has an extremum precisely, provided that

$$1-f(R_{\text{turn}}) > 0, \quad G(R_{\text{turn}}) = 0, \quad G'(R_{\text{turn}}) > 0, \quad (10)$$

where R_{turn} denotes the star-surface radius at which the apparent-horizon curve turns. Since Eq. (9) and Eq. (10) hold in a neighborhood of R_{turn} , it follows that dR_{AH}/dT switches from negative to positive as T increases. Therefore $R_{\text{AH}}(T)$ has a *local minimum*, which we call a *left vertex*. Such non-monotonic behavior is absent in the Schwarzschild collapse but may arise in more general exteriors with two horizons, as we will demonstrate explicitly for the RN collapse in Section 4.

Using the Misner-Sharp mass function $m(R)$ [10],

$$f(R) = 1 - \frac{2m(R)}{R}, \quad (11)$$

a turning point of $R_{\text{AH}}(T)$ occurs at the star-surface radius $R = R_{\text{turn}}$ when

$$\frac{dR_{\text{AH}}}{dT} = 0 \iff m'(R_{\text{turn}}) R_{\text{turn}} - 3m(R_{\text{turn}}) = 0, \quad m(R_{\text{turn}}) > 0. \quad (12)$$

It is clear that such a left vertex is absent for the Schwarzschild exterior. We shall discuss the condition when it could arise and the constraints on the consistency of the generalized OS collapse.

3.2 Star-surface bounce

On the collapsing OS surface ($\dot{R} < 0$), Eq. (5) implies that the motion is real only when $f(R) \leq 1$. It follows from (5) that a turning point could occur when the collapse stops at some

finite and nonzero R_* , namely

$$\dot{R}(R_*) = 0 \quad \iff \quad f(R_*) = 1. \quad (13)$$

It is clear that such an R_* does not exist in the Schwarzschild case. A *bounce* means that $R(T)$ attains a local minimum at R_* and reverses into expansion, i.e. $\ddot{R}(R_*) > 0$. Differentiating (5) yields the exact identity

$$\ddot{R} = -\frac{d}{dT} \sqrt{1 - f(R)} = -\frac{1}{2} f'(R), \quad (14)$$

so a turning point is a bounce precisely when

$$f(R_*) = 1, \quad f'(R_*) < 0. \quad (15)$$

It is also useful to express the bounce criterion in terms of the Misner-Sharp mass function. The allowed region becomes $m(R) \geq 0$, while the turning point (13) and the bounce condition (15) imply the existence of R_* such that

$$m(R_*) = 0, \quad m'(R_*) > 0. \quad (16)$$

Therefore, a surface bounce can occur only if the exterior develops an inner forbidden pocket with $f(R) > 1$ (or $m(R) < 0$) for $0 < R < R_*$, which we refer to as an RN-type repulsive core. As we shall see later, the requirement that $m'(R_*) > 0$ is ensured by the null energy condition (NEC).

There is also another special radius during the collapse that is worth paying attention. Before the surface stops and reverses at R_* , there must already exist an *inflection radius* R_{infl} where the collapse changes from accelerating to decelerating. This inflection point satisfies

$$\ddot{R}(R_{\text{infl}}) = 0 \quad \iff \quad f'(R_{\text{infl}}) = 0, \quad (17)$$

with $\dot{R}(R_{\text{infl}}) \neq 0$. At R_{infl} the surface is still collapsing, but its acceleration switches sign. Note that this inflection radius R_{infl} is generally different from the apparent-horizon turning point R_{turn} defined by (12).

Considering the case where the exterior spacetime admits two horizons, $0 < R_- < R_+$, such that $f(R_{\pm}) = 0$, we suppose the case that OS surface undergoes a bounce at $R_* > 0$, meaning that R_* is the inner boundary of the allowed region and satisfies

$$f(R_*) = 1, \quad f(R) > 1 \quad \text{for all } 0 < R < R_*. \quad (18)$$

Since $f(R_-) = 0$ and $R_- > 0$, the point R_- would belong to the interval $(0, R_*]$ if one assumed $R_* \geq R_-$. However, the defining property of a bounce requires $f(R) > 1$ for every $0 < R < R_*$, which in particular would imply $f(R_-) > 1$. This contradicts $f(R_-) = 0$. Therefore, any bouncing point lies inside the inner horizon, i.e.,

$$R_* < R_-. \quad (19)$$

3.3 Interplay between the bounce and the left vertex

The local criteria for a left vertex (12) and a surface bounce (15) are independent. However, in a standard asymptotically flat OS collapse starting from a sufficiently large initial radius, a bounce enforces the existence of a left vertex along the collapsing star surface, but the converse may not be true.

Bounce \Rightarrow a left vertex. Along the collapsing surface, the apparent-horizon slope is given by,

$$\frac{dR_{\text{AH}}}{dT} = \frac{m'(R)R - 3m(R)}{2m(R)}. \quad (20)$$

Asymptotic flatness implies $m(R) \rightarrow M$ and $m'(R) \rightarrow 0$ as $R \rightarrow \infty$, hence $\frac{dR_{\text{AH}}}{dT} \rightarrow -\frac{3}{2} < 0$ at early stages of collapse. If the surface undergoes a bounce at $R_* > 0$, namely $m(R_*) = 0$ with $m'(R_*) > 0$, then as $R \rightarrow R_*^+$ the numerator approaches $m'(R_*)R_* > 0$ while the denominator $2m(R) \rightarrow 0^+$, so $\frac{dR_{\text{AH}}}{dT} \rightarrow +\infty$. By continuity, there must exist a $R_{\text{turn}} \in (R_*, R_0)$ such that

$$\left. \frac{dR_{\text{AH}}}{dT} \right|_{R_{\text{turn}}} = 0, \quad (21)$$

which yields a left vertex on the collapsing star surface.

Vertex without bounce. Conversely, a left vertex may occur without any bounce. It suffices to choose an asymptotically flat mass profile with $m(R) > 0$ for all $R > 0$, while $m'(R)R - 3m(R)$ changes sign. A simple analytic example is

$$m(R) = M \left(1 - e^{-(R/L)^p} \right), \quad M > 0, \quad L > 0, \quad p > 3. \quad (22)$$

It is clear that $m(R) > 0$ for all $R > 0$ and $m(R) \rightarrow M$ as $R \rightarrow \infty$, so no bounce occurs. Meanwhile, the quantity $m'(R)R - 3m(R) = M[(px + 3)e^{-x} - 3]$ with $x = (R/L)^p$ is positive for small R (since $p > 3$) and it approaches $-3M$ as $R \rightarrow \infty$. Thus, the quantity vanishes at some finite $R_{\text{turn}} > 0$. By (20), this produces a left vertex of $R_{\text{AH}}(T)$.

4 RN collapse: a bounce with a vertex

The RN geometry provides a simple explicit example of a static exterior that can exhibit *both* signature features discussed in Section 3: a bounce of the star surface and a left vertex in the apparent-horizon trajectory. The RN exterior spacetime is described by

$$f_{\text{RN}}(r) = 1 - \frac{2m}{r} + \frac{q^2}{r^2}, \quad (23)$$

where m and q denote the mass and the electric charge. The corresponding Misner–Sharp mass function is

$$m(r) = m - \frac{q^2}{2r}. \quad (24)$$

For $0 < |q| < m$ there are two horizons,

$$R_{\pm} = m \pm \sqrt{m^2 - q^2}, \quad (25)$$

with R_+ the radius of the outer horizon and R_- the inner horizon; the extremal limit $|q| = m$ gives $R_+ = R_- = m$. Throughout this section we restrict to the black hole parameter $0 < |q| \leq m$ and assume the OS collapse starts from a sufficiently large initial radius $R_0 > R_+$.

4.1 Apparent-horizon vertex

Substituting (24) into the general vertex condition (12) yields

$$R_{\text{turn}} = \frac{2q^2}{3m}. \quad (26)$$

This vertex is dynamically accessible since

$$1 - f_{\text{RN}}(R_{\text{turn}}) = \frac{3m^2}{4q^2} > 0. \quad (27)$$

For a physically consistent black-hole formation, the inner apparent-horizon should connect the outer and inner horizons as the star’s surface crosses them. In the (R, T) diagram, the apparent-horizon trajectory is the parametric curve $(R_{\text{AH}}(R), T(R))$, so the vertex is located at $(R_{\text{AH}}(R_{\text{turn}}), T(R_{\text{turn}}))$, where R_{turn} is determined by $dR_{\text{AH}}/dT = 0$. The inner-horizon crossing of the surface occurs at the point $(R_-, T(R_-))$. Since $R_{\text{AH}}(R_-) = R_-$ and the vertex is the *minimum* of $R_{\text{AH}}(T)$ along the collapsing star surface, its horizontal coordinate automatically satisfies $R_{\text{AH}}(R_{\text{turn}}) \leq R_-$. The nontrivial requirement is therefore the correct *time ordering*: the vertex must occur no earlier than the crossing of the apparent horizon over the inner horizon,

$$T(R_{\text{turn}}) \geq T(R_-). \quad (28)$$

On the collapsing star surface, we have $\frac{dT}{dR} = -\frac{1}{\sqrt{1-f(R)}} < 0$, so $T(R)$ increases monotonically as R decreases. Hence (28) is equivalent to the simple radial condition

$$R_{\text{turn}} \leq R_-, \quad (29)$$

where $R_{\pm} = m \pm \sqrt{m^2 - q^2}$ are the RN horizon radii. Together with $q^2 \leq m^2$, we obtain the consistent range on the charge q

$$\frac{\sqrt{3}}{2}m \leq |q| \leq m. \quad (30)$$

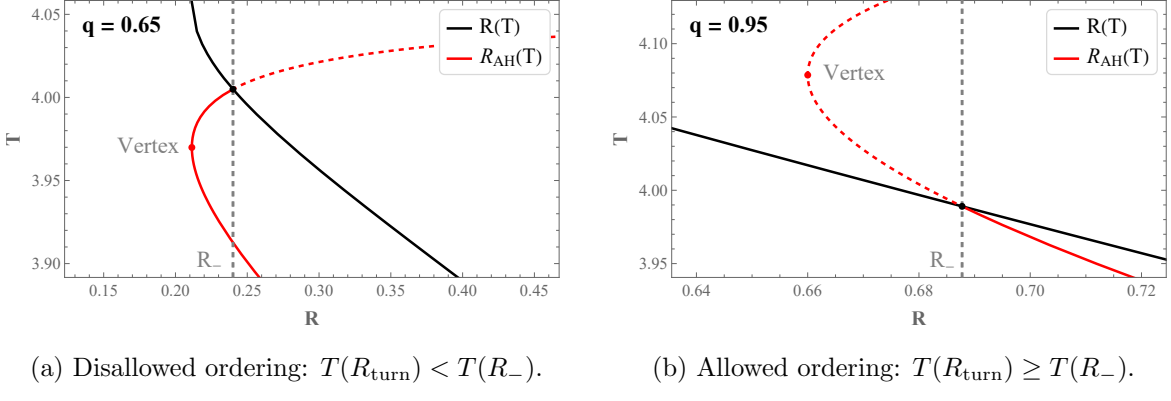


Figure 1: Depending on the charges, two possible time orderings between the apparent-horizon turning point and the inner-horizon crossing in RN OS collapse with $m = 1$ (left: $q = 0.65$; right: $q = 0.95$). The black curve is the star-surface trajectory $(R, T(R))$, while the red curve is the apparent-horizon trajectory $(R_{\text{AH}}(R), T(R))$. The condition (29) is a global consistency requirement: it ensures that the relevant inner apparent-horizon evolution connects smoothly to the surface crossing of the inner horizon; otherwise, the turning occurs too early, while the surface is still outside R_- .

In particular, when $q^2 = 3m^2/4$, we have $R_{\text{turn}} = R_-$. In Fig. 1, we illustrate the consistent and inconsistent vertex structures in the OS collapse. The left panel is associated with a small charge so that the vertex occurs at T , when the star surface $R_{\text{turn}} = R(T) > R_-$. Consequently particles can move outward in the would-be trapped region, defined by the enclosed region by the apparent horizon and star surface. This is certainly contradictory. Such contradiction disappears for sufficiently large charge, where the vertex occurs at R_{turn} that is outside the trapped region.

4.2 Star-surface bounce

In the RN black hole, the charge contribution produces an inner repulsive barrier, so the OS surface can reach a *bounce radius*. On the collapsing star surface, the bounce radius R_* is determined by $f_{\text{RN}}(R_*) = 1$, which gives

$$R_* = \frac{q^2}{2m}. \quad (31)$$

To confirm that R_* is a bounce, we use the general relation in Eq. (14). For the RN metric,

$$f'_{\text{RN}}(R_*) = -\frac{8m^3}{q^4} < 0 \implies \ddot{R}(R_*) = \frac{4m^3}{q^4} > 0, \quad (32)$$

so the surface reaches R_* with vanishing velocity and positive outward acceleration, and therefore rebounds. This bounce occurs for all $0 < |q| \leq m$, and one has the ordering

$$R_* < R_- < R_+. \quad (33)$$

Thus we see that in the framework of the OS evolution, the star surface never reaches $R = 0$; instead, it bounces back to the inner horizon. This implies that the inner horizon is unstable since it lies between the trapped and bounce regions. The OS collapse indicates that singularity will actually develop on the inner horizon, consistent with SCCC.

4.2.1 Surface trajectory and near-bounce behavior

On the collapsing star surface, the OS surface satisfies Eq. (5), hence

$$\frac{dT}{dR} = -\frac{1}{\sqrt{1 - f_{\text{RN}}(R)}} = -\frac{R}{\sqrt{2mR - q^2}}. \quad (34)$$

Imposing the initial condition $T(R_0) = 0$, the surface worldline in the (R, T) plane can be written schematically as

$$T(R) = \begin{cases} \frac{(mR_0 + q^2)\sqrt{2mR_0 - q^2} - (mR + q^2)\sqrt{2mR - q^2}}{3m^2}, & (R_* \leq R \leq R_0), \quad \text{collapse} \\ 2T_* - \frac{(mR_0 + q^2)\sqrt{2mR_0 - q^2} - (mR + q^2)\sqrt{2mR - q^2}}{3m^2}, & (R_* \leq R \leq R_-), \quad \text{bounce} \end{cases} \quad (35)$$

where $T_* \equiv T(R_*)$ denotes the proper time at the bounce radius $R_* = q^2/(2m)$. The two branches join smoothly at the bounce point (R_*, T_*) .

Moreover, the bounce is locally regular. Expanding $f_{\text{RN}}(r)$ around $r = R_*$ gives $1 - f_{\text{RN}}(R) \simeq -f'_{\text{RN}}(R_*)(R - R_*)$ with $f'_{\text{RN}}(R_*) < 0$, so that the surface radius has a quadratic minimum,

$$R(T) = R_* + \frac{2m^3}{q^4} (T - T_*)^2 + \mathcal{O}((T - T_*)^4). \quad (36)$$

After the surface crosses the outer horizon R_+ , it enters the trapped region $R_- < R < R_+$, where the causal structure prevents any outward escape back to the original exterior. In the idealized OS evolution on a fixed RN background one may formally continue the trajectory to $R < R_-$ and reach the bounce radius R_* , but in a realistic collapse this continuation is not expected to be physically meaningful: the star effectively gets “captured” by the inner horizon. This is closely tied to the well-known instability of the inner horizon, which suggests that the inner horizon should not survive as a regular boundary in dynamical collapse—in the spirit of Penrose’s viewpoint [9] that an extendible inner horizon would signal a breakdown of determinism and should instead be replaced by a singular endpoint.

The inner horizon is known to be unstable due to mass inflation [13]: even tiny perturbations can trigger an exponential growth of the local effective mass, potentially leading to a weak, null curvature singularity at or just inside $R = R_-$. In that case, the classical space-like singularity at $R = 0$ may never form within the dynamical evolution, or it may become causally disconnected and physically irrelevant, with the effective endpoint occurring near the

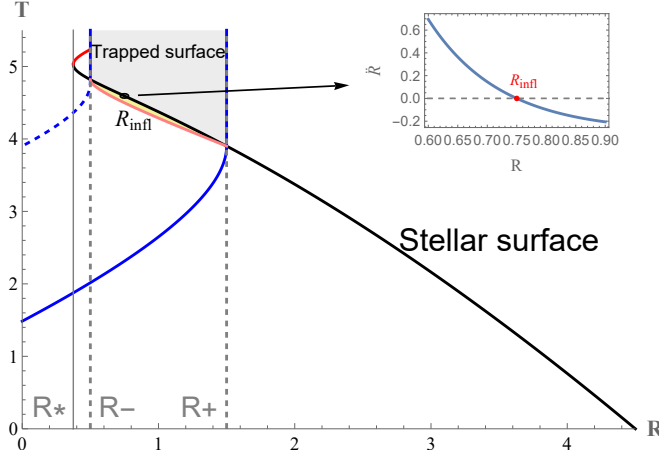


Figure 2: RN collapse in the (R, T) plane. The initial radius is $R_0 = 4.5$, and the inner and outer horizons are set to $(R_-, R_+) = (0.5, 1.5)$. These choices fix the mass and charge as $m = (R_+ + R_-)/2 = 1$ and $q^2 = R_+ R_- = 0.75$. The collapse features three key radii: the surface bounce radius $R_* = 0.375$, the apparent-horizon vertex $R_{\text{turn}} = 0.5 = R_-$, and the inflection point $R_{\text{infl}} = 0.75$. The black curve shows the star surface $R(T)$. The blue and red curves denote the apparent horizon and event horizon, respectively. The trapped regions are shaded.

inner horizon instead. It should also be noted that the consistency interval (30) ensures that the bounce radius R_* is not parametrically small and is therefore a physically meaningful feature.

To complete the picture of RN collapse, we also consider the *inflection point* R_{infl} , where the surface acceleration vanishes, i.e. $\ddot{R} = 0$, which gives

$$R_{\text{infl}} = \frac{q^2}{m}. \quad (37)$$

Note that $R_{\text{infl}} = 2R_*$, so it lies outside the bounce radius. At this point, the surface is still collapsing, with $\dot{R}(R_{\text{infl}}) = -m/|q| \neq 0$. However, the acceleration changes sign: collapse speeds up for $R > R_{\text{infl}}$ ($\ddot{R} < 0$) and slows down for $R < R_{\text{infl}}$ ($\ddot{R} > 0$) until the bounce occurs at R_* . The apparent-horizon vertex radius $R_{\text{turn}} = 2q^2/(3m)$ lies between the bounce and inflection points,

$$R_* = \frac{q^2}{2m} < R_{\text{turn}} = \frac{2q^2}{3m} < R_{\text{infl}} = \frac{q^2}{m}. \quad (38)$$

In Fig. 2, we draw the diagram of OS collapse of the RN black holes with sufficiently large charge so that there is no left vertex of the apparent horizon before it crosses over the inner horizon. We illustrate the inflection radius, after which the star surface decelerates and then bounce back to the inner horizon. The matter accumulation in the inner horizon indicates that it is unstable, consistent with Penrose's SCCC.

5 Regular black hole collapse

In the previous sections, we have seen that the OS collapse of black holes with additional inner horizon such as the RN black hole can have new features, such as the bounce of the star surface inside the inner horizon and also the possible existence of the left vertex of the apparent horizon. However, having two horizons is only a necessary, but not sufficient condition for these new features. Regular black holes necessarily have two horizons, but the analysis of the OS collapse of the Bardeen black hole illustrates that there is neither bounce nor vertex [12]. In this section, we show that this is in fact generally true for regular black holes. It turns out that this observation allows us to give a new proof that regular black hole with a Minkowski core necessarily violates the NEC.

5.1 Regular black holes: no bounce or vertex

A regular black hole with the special static metric (2) is characterised by a regular core, which can be de Sitter (dS), anti-de Sitter (AdS) or Minkowski. It was shown that such regular black holes satisfying the NEC must have a de Sitter core [14]. Requiring NEC also implies that the regular black hole must have $f(r) \leq 1$, with inequality saturated at both asymptotic infinity ($r \rightarrow \infty$) and at the core ($r = 0$). It is then clear that there can be no bounce, since a necessary condition for bounce is the existence of a finite R_* such that $f(R_*) = 1$. Furthermore, as the collapsing star-surface radius R approaches the core asymptotically, namely

$$R \sim e^{-T/\tau_0}, \quad \tau_0 = \sqrt{\frac{3}{\Lambda_{\text{eff}}}}, \quad (39)$$

where Λ_{eff} is the effective cosmological constant of the dS core. The asymptotic behavior yields what we call a *soft-landing* collapsing scenario. An explicit concrete example is given in Appendix A.

In the previous RN example, we have also seen that apparent-horizon vertex can arise; However, when the charge is too small, the left vertex lies inside the star, making the OS collapse inconsistent. This inconsistency disappears for sufficiently large charge. We now show that apparent-horizon vertex will never arise in the OS collapse of regular black holes satisfying the NEC. To see this, we consider the exterior metric profile (2) and define the Misner-Sharp mass $m(r)$. We require that the exterior matter satisfies the NEC, which for (2) implies

$$\frac{1}{2}f''(r) + \frac{1-f(r)}{r^2} \geq 0. \quad (40)$$

In Misner-Sharp language, this becomes

$$\frac{1}{2}f''(r) + \frac{1-f(r)}{r^2} = \frac{2m'(r) - r m''(r)}{r^2} \geq 0 \quad \iff \quad \frac{d}{dr} \left(\frac{m'(r)}{r^2} \right) \leq 0, \quad (41)$$

so $m'(r)/r^2$ is nonincreasing outward. Suppose in addition that the center is regular in the sense that

$$m(0) = 0, \quad m(r) = \mathcal{O}(r^3) \quad (r \rightarrow 0). \quad (42)$$

Then for any $r > 0$ and all $0 < x < r$ one has

$$\frac{m'(x)}{x^2} \geq \frac{m'(r)}{r^2} \quad \Rightarrow \quad m'(x) \geq \frac{m'(r)}{r^2} x^2. \quad (43)$$

Integrating from $x = 0$ to $x = r$ yields the inequality

$$m(r) = \int_0^r m'(x) dx \geq \frac{m'(r)}{r^2} \int_0^r x^2 dx = \frac{r m'(r)}{3}, \quad \Rightarrow \quad 3m(r) - r m'(r) \geq 0. \quad (44)$$

Recalling $G(r) = r f'(r) + 2(1 - f(r)) = \frac{2}{r}(3m(r) - r m'(r))$, we obtain $G(r) \geq 0$. Along the physically allowed collapsing star surface ($1 - f(R) \geq 0$), Eq. (9) gives

$$\frac{dR_{\text{AH}}}{dT} = -\frac{G(R)}{2(1 - f(R))} \leq 0. \quad (45)$$

Therefore, $R_{\text{AH}}(T)$ is monotone and cannot develop a left vertex. Note that this conclusion relies crucially on regularity at the center and does not apply to singular exteriors such as RN, for which $m(r)$ is not integrable at $r = 0$ and $3m - rm'$ can change sign.

5.2 Regular core-based classification

We now classify regular-core exteriors by their near-origin expansion of $f(r)$ and discuss for each core type whether a left vertex or a bounce is expected. For the special static metric of the type (2), there can be three different types of regular cores: dS, AdS and Minkowski cores. The AdS core requires SEC, in which case, it can be shown that the core cannot be extended to asymptotic Minkowski infinity [14]. We thus consider the dS core:

$$f(r) = 1 - \frac{\Lambda_{\text{eff}}}{3} r^2 + \mathcal{O}(r^4) \quad (r \rightarrow 0), \quad (\Lambda_{\text{eff}} > 0). \quad (46)$$

We have

$$m(r) = \frac{r}{2}(1 - f(r)) = \frac{\Lambda_{\text{eff}}}{6} r^3 + \mathcal{O}(r^5), \quad m'(r) = \frac{\Lambda_{\text{eff}}}{2} r^2 + \mathcal{O}(r^4). \quad (47)$$

Hence $m'(r)r - 3m(r) = \mathcal{O}(r^5)$ and Eq. (20) gives $dR_{\text{AH}}/dT \rightarrow 0$ as $R \rightarrow 0$. This near-core flattening alone does not exclude a finite-radius turning point. However, if the exterior satisfies the NEC on the relevant accessible region, then we have shown that $dR_{\text{AH}}/dT \leq 0$ throughout the collapse and thus excludes any left vertex. In fact, it is easy to verify that R_{AH} approach to the constant τ_0 , given in (39), asymptotically in large proper time T . We illustrate these features in the OS collapse of the electrically-charged regular black hole of EMS gravity in Appendix A.

Regular black holes with Minkowski core on the other hand *have at least one left vertex* provided the collapsing surface can probe sufficiently small radii while remaining in the allowed region ($m > 0$). It does not generically produce a bounce. For example, considering

$$f(r) = 1 - c_4 r^4 + \mathcal{O}(r^6) \quad (r \rightarrow 0), \quad (c_4 > 0), \quad (48)$$

we have $m(r) = \frac{c_4}{2} r^5 + \mathcal{O}(r^7)$ and $m'(r) = \frac{5c_4}{2} r^4 + \mathcal{O}(r^6)$, hence

$$m'(r) r - 3m(r) = c_4 r^5 + \mathcal{O}(r^7) > 0 \implies \frac{dR_{\text{AH}}}{dT} \rightarrow 1 > 0 \quad (R \rightarrow 0). \quad (49)$$

On the other hand, asymptotic flatness implies $m(R) \rightarrow M$ and $m'(R) \rightarrow 0$ as $R \rightarrow \infty$, so $\frac{dR_{\text{AH}}}{dT} \rightarrow -\frac{3}{2} < 0$ at early stages. Therefore $\frac{dR_{\text{AH}}}{dT}$ must vanish at least once at some intermediate R_{turn} by continuity, yielding a left vertex of $R_{\text{AH}}(T)$ on the infalling evolution. Although we only considered a specific example to illustrate the point, the statement is generally true for all regular black holes with a Minkowski core. Combined with the statement that regular black holes satisfying NEC can never have a left vertex, we thus give a new proof that regular black holes with Minkowski core necessarily violate the NEC. This theorem was also proved in [14] using a different method.

6 Conclusion

In this paper, we studied the generalized OS collapse of non-Schwarzschild black holes, focusing on those with two horizons, inner Cauchy and outer event horizons. The OS collapse with the FLRW interior requires the exterior metric to be special static metrics of the type (2). We found that new features could arise when a black hole has two horizons. The first is a *left vertex* in the apparent-horizon evolution. Along the collapsing surface, the apparent-horizon radius $R_{\text{AH}}(T)$ can have a temporary minimum. This behavior is controlled by the local turning-point conditions in Eqs. (9)-(10) (or equivalently Eq. (12)). The second is a *bounce* at a nonzero radius of the star's surface. In terms of $f(r)$, this occurs when $f(R_*) = 1$ with $f'(R_*) < 0$ (Eq. (15)), ensuring that the turning point is a local minimum of $R(T)$. Equivalently, the Misner-Sharp mass $m(r)$ crosses zero from below, indicating an inner repulsive barrier that reflects the collapsing surface. Such a bounce is excluded in Schwarzschild metric and, more generally, in exteriors with $m(r) \geq 0$ for all $r > 0$. We also highlighted an effect, the *inflection radius* R_{infl} defined by $\ddot{R}(R_{\text{infl}}) = 0$, where the collapse switches from accelerating to decelerating while remaining on the collapsing star surface, before the bouncing taking place.

For the RN exterior, we explicitly showed that the OS collapse exhibited both new features. Requiring the apparent-horizon turning point to lie inside the inner horizon ($R_{\text{turn}} \leq R_-$) forces

the charge to be sufficiently large, which also ensures that the bounce scale is not parametrically small. Thus, RN collapse provides a clean analytic benchmark featuring three distinct radii:

- $R_* = q^2/(2m)$: the surface stops and bounces ($\dot{R} = 0, \ddot{R} > 0$);
- $R_{\text{infl}} = q^2/m$: the collapse changes from accelerating to decelerating ($\dot{R} \neq 0, \ddot{R} = 0$);
- $R_{\text{turn}} = 2q^2/(3m)$: the apparent horizon reaches a minimum (vertex condition (12)).

However, the existence of both inner and outer horizons does not necessarily imply that the two new features must occur in the OS collapse. In fact, for regular black holes, which necessarily have two horizons, their OS collapse has no apparent-horizon left vertex, nor any bounce. Instead, the collapse exhibits a soft landing: the surface approaches $R \rightarrow 0$ only asymptotically in proper time, while $R_{\text{AH}}(R)$ tends to a finite limiting radius. Furthermore, the NEC-based monotonicity result for regular centers implies a monotone apparent-horizon trajectory and excludes any left vertex. This allows to prove a no-go theorem that regular black holes with Minkowski core necessarily violate the NEC. We explicitly illustrate the OS collapse of regular black holes in EMS in Appendix A. As another explicit example, we showed in Appendix B that the critical Einstein-Born-Infeld exterior also exhibits neither a bounce nor a vertex.

We now summarize the qualitative behaviors of the star surface $R(T)$ in the OS collapse for black holes with at most two horizons. The collapse leads to one of three possible outcomes:

- **Singular collapse (e.g. Schwarzschild):** The surface reaches $R = 0$ in finite proper time. After trapped surfaces form, the apparent-horizon radius $R_{\text{AH}}(T)$ decreases monotonically and terminates at the center at the final collapse time.
- **Bouncing collapse (e.g. RN):** The surface stops at a finite radius R_* and reverses into expansion. In a standard asymptotically flat OS evolution starting from sufficiently large R_0 , a bounce may be accompanied by a turning behavior of $R_{\text{AH}}(T)$; in fact, under standard asymptotically flat OS initial data, a bounce implies at least one left vertex (see Sec. 3.3). Both the surface and the apparent horizon show this turning behavior because of the same repulsive effect in the spacetime.
- **Soft-landing collapse (e.g. regular black holes):** The star never reaches the center in finite time; it only gets closer and closer as time goes to infinity. The apparent horizon also changes smoothly and never turns around. Neither the surface nor the horizon shows a bounce or a vertex.

Thus, by inspecting how the star surface and the apparent horizon behave, we can tell which type of collapse is actually occurring.

Our results may provide an insight of the (in)stability of the inner horizon that is relevant to SCCC. For the RN black hole with a timelike singularity, the bounce of the OS collapse indicates that matter accumulates on the horizon and hence it is unstable. For regular black holes, the existence of the inner horizon may not violate SCCC, and interestingly, there will be no bounce in the OS collapse.

In this paper, we considered special static black holes with at most two horizons. We found that three outcomes could arise in OS collapse. Black holes with multiple horizons beyond two could arise when the SEC is violated [17]. It is of great interest to investigate the fate of the OS collapse in these more complicated cases.

Acknowledgements

We are grateful to Fatimah Shojai for useful discussions. This work is supported in part by the National Natural Science Foundation of China (NSFC) grants No. W2533015 No. 12375052 and No. 11935009, as well as by the Tianjin University Self-Innovation Fund Extreme Basic Research Project Grant No. 2025XJ21-0007.

Appendix A OS collapse of regular EMS black holes

Since Bardeen constructed the first example of the regular black hole metric, there have been efforts in constructing fundamental theories that admit such regular black holes. Notable examples include Einstein gravity coupled to the nonlinear electrodynamics, (e.g. [14, 18–20]) and quasi-topological pure gravity theory, e.g. [21]. In this appendix, we present an explicit example of the OS collapse of electrically-charged regular black holes in EMS gravity. We also present a representative collapse diagram, illustrating explicitly the absence of both a surface bounce and an apparent-horizon left vertex, in agreement with the discussion in Section 5.

We consider the EMS theory with action

$$S = \frac{1}{16\pi} \int d^4x \sqrt{-g} (R - \phi^{-1} \mathcal{F} - V(\phi)), \quad (50)$$

where $\mathcal{F} \equiv \frac{1}{4} F_{\mu\nu} F^{\mu\nu}$ and $F_{\mu\nu} = \partial_\mu A_\nu - \partial_\nu A_\mu$. The scalar ϕ is auxiliary (no kinetic term); its algebraic equation of motion relates ϕ to \mathcal{F} . Eliminating ϕ yields an effective nonlinear electrodynamics in the usual F -framework. The auxiliary scalar field form (50) is convenient for organizing solution branches and imposing regularity at the core.

As an explicit solvable example we take the V_1 family [11]. For general (n, α) one has

$$V_1(\phi) = \frac{1}{\alpha} \left(1 - \phi^{\frac{n}{n+1}}\right)^{\frac{n+1}{n}}, \quad (51)$$

$$f(r) = 1 - \frac{2m}{r} + \frac{q^2}{4r^2} {}_2F_1\left(\frac{1}{4n}, \frac{1}{n}; 1 + \frac{1}{4n}; -\left(\frac{\alpha q^2}{2r^4}\right)^n\right). \quad (52)$$

The solution involves two independent parameters, the mass m and the charge q . The solution is generally singular, but regularity at the origin can be realized on the critical branch, namely $m = m_{\text{cr}}(q)$, where the would-be $1/r$ term cancels in the small- r expansion and the geometry develops a dS core. For instance, for $(n, \alpha) = (1, 1)$ and $q = 15$ we find numerically $m = m_{\text{cr}}(15) \approx 9.592$, and the resulting geometry has two horizons at

$$R_- \simeq 2.655, \quad R_+ \simeq 15.574. \quad (53)$$

In this example one verifies numerically that $f(r) < 1$ for all $r > 0$, so no surface turning point satisfying $f(R_*) = 1$ with $f'(R_*) < 0$ exists (hence no bounce). Moreover, the effective density $\rho_{\text{ext}}(r)$ decreases outward on $0 < r < R_+$, which implies $dR_{\text{AH}}/dT < 0$ along the collapsing branch and therefore we have a monotone apparent-horizon curve with no left vertex, consistent with the discussion in Section 5. Relevant diagram is plotted in Fig. 3. In particular, we see explicitly that there exists inflection point where the collapse transit from the accelerating phase to the decelerating phase. Nevertheless, there is no bounce of the star surface, which monotonically collapses to the core only asymptotically in the proper time.

Appendix B OS collapse of critical Born-Infeld black hole

We show that the Einstein-Born-Infeld (EBI) exterior, when in critical mass/charge relation, provides another concrete example of a non-Schwarzschild spacetime with *neither* an apparent-horizon left vertex nor a bounce. For a purely electric EBI black hole the theory is of $L(\mathcal{F})$ type [15, 16],

$$L(\mathcal{F}) = \frac{4}{\alpha} \left(1 - \sqrt{1 + \frac{\alpha}{2} \mathcal{F}}\right), \quad \alpha > 0, \quad (54)$$

where α sets the Born-Infeld scale. The theory admits charged black hole solution of the ansatz (2), with f given by

$$f_{\text{BI}} = 1 - \frac{2M}{r} + \frac{2r^2}{3\alpha} \left(1 - {}_2F_1\left[-\frac{3}{4}, -\frac{1}{2}, \frac{1}{4}, -\frac{\alpha q^2}{4r^4}\right]\right). \quad (55)$$

For generic mass and charge (M, q) , the small- r expansion of $f_{\text{BI}}(r)$ contains a $1/r$ term. The metric has time-like singularity, as in the case of the RN black hole. Thus in the general cases, there will be both bounce and apparent-horizon vertex.

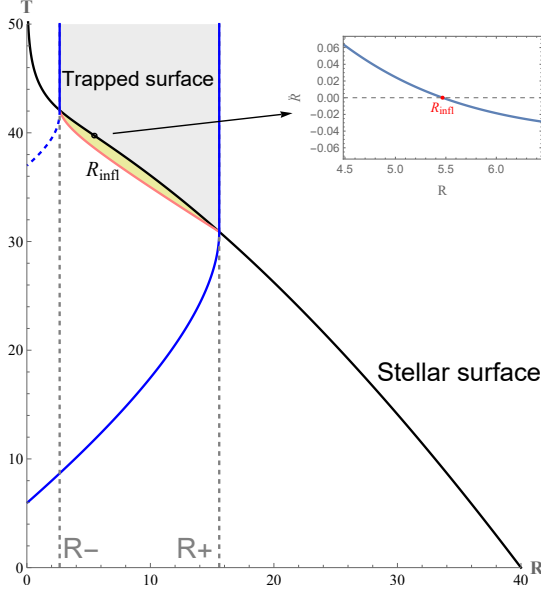


Figure 3: Collapse diagram in the (R, T) plane for a electrically-charged regular black hole in EMS gravity with $(n, \alpha) = (1, 1)$ and $(q, m) = (15, m_{\text{cr}}(15))$, starting from $R_0 = 40$. The vertical lines indicate the horizon radii R_{\pm} in (53). The star surface $R(T)$ (black) exhibits no turning point and thus no bounce. The apparent-horizon curve $R_{\text{AH}}(T)$ (pink) is monotone and has no left vertex. The inflection radius $R_{\text{infl}} \simeq 5.47$ is defined by $\ddot{R} = 0$: the collapse accelerates in the $R > R_{\text{infl}}$ region and decelerates in the $R < R_{\text{infl}}$ region, consistent with the soft-landing behavior as $R \rightarrow 0$.

We are interested in the case where the $1/r$ term vanishes by requiring its cancellation selects a distinguished critical mass $M = M_{\text{cr}}$, where

$$M_{\text{cr}} = \frac{q^{3/2} \Gamma(\frac{1}{4})^2}{12\sqrt{2\pi} \alpha^{1/4}}, \quad (56)$$

for which the core is less singular. On this critical branch the near-origin expansion reads

$$f_{\text{BI}}(r) = 1 - \frac{q}{\sqrt{\alpha}} + \frac{2}{3\alpha} r^2 + \mathcal{O}(r^4), \quad (r \rightarrow 0), \quad (57)$$

so in general $f_{\text{BI}}(0) = 1 - q/\sqrt{\alpha} \neq 1$. In Misner–Sharp language one finds

$$m(r) = \frac{r}{2} (1 - f_{\text{BI}}(r)) = \frac{q}{2\sqrt{\alpha}} r - \frac{1}{3\alpha} r^3 + \mathcal{O}(r^5), \quad (r \rightarrow 0), \quad (58)$$

hence $m(r) > 0$ for sufficiently small $r > 0$, and the OS reality condition $m(R) \geq 0$ holds near the center.

No left vertex and no bounce. By the vertex criterion derived in Section 3, a left vertex can occur only if the apparent-horizon slope along the collapsing surface vanishes at some accessible radius. On the critical EBI branch this never happens. Indeed, the regular-core

expansion (57) implies $G(r) = \frac{2q}{\sqrt{\alpha}} + \mathcal{O}(r^4) > 0$ as $r \rightarrow 0^+$, while asymptotic flatness gives $G(r) = \frac{6M_{\text{cr}}}{r} - \frac{q^2}{r^2} + \dots > 0$ as $r \rightarrow \infty$. Using the explicit critical EBI profile, one furthermore verifies that $G(r)$ remains strictly positive for all $r > 0$ on the accessible branch. Since $1 - f(r) > 0$ holds along the collapse, Eq. (9) then yields $dR_{\text{AH}}/dT < 0$ throughout the evolution, so $R_{\text{AH}}(T)$ is monotone and admits no left vertex.

A bounce requires an inner forbidden pocket $f(r) > 1$ and a first turning point $R_* > 0$ where $f(R_*) = 1$ with $f'(R_*) < 0$; see Section 3.2. This is impossible on the critical EBI branch because $f_{\text{BI}}(r) \leq 1$ holds throughout the accessible region. Therefore the collapsing surface encounters no turning point and no bounce occurs.

References

- [1] J.R. Oppenheimer and H. Snyder, “On continued gravitational contraction,” *Phys. Rev.* **56** (1939) 455–459, doi:10.1103/PhysRev.56.455.
- [2] W. Israel, “Singular hypersurfaces and thin shells in general relativity,” *Nuovo Cim. B* **44S10** (1966) 1 [erratum: *Nuovo Cim. B* **48** (1967) 463], doi:10.1007/BF02710419.
- [3] Z.C. Li, H. Khodabakhshi and H. Lü, “The upper bound of event horizon formation time in generalized Oppenheimer-Snyder collapse,” [arXiv:2512.24421 [gr-qc]], to appear in PLB.
- [4] J. Bardeen, “Nonsingular general relativistic gravitational collapse,” in Proceedings of the International Conference GR5, Tbilisi, U.S.S.R. (1968), p. 174.
- [5] S.A. Hayward, “Formation and evaporation of non-singular black holes,” *Phys. Rev. Lett.* **96** (2006) 031103, doi:10.1103/PhysRevLett.96.031103, [arXiv:gr-qc/0506126 [gr-qc]].
- [6] H. Khodabakhshi, H. Lü and F. Shojai, “Gravitational collapse: generalizing Oppenheimer Snyder and a conjecture on horizon formation time,” *Phys. Rev. D* **12** (2025) 124057, doi:10.1103/PhysRevD.112.124057, [arXiv:2506.03702 [gr-qc]].
- [7] R. Penrose, *Singularities of Spacetime, Theoretical Principles in Astro physics and Relativity* (A78-43851 19-90), Chicago University Press, Chicago, 1978.
- [8] S.W. Hawking, W. Israel, *General Relativity, an Einstein Centenary Survey*, Cambridge University Press, Cambridge, 1979.
- [9] R. Penrose, “The question of cosmic censorship,” *Gen. Rel. Grav.* **34** (2002) 1141, doi:10.1023/A:1016346228772.

[10] C.W. Misner and D.H. Sharp, “Relativistic equations for adiabatic, spherically symmetric gravitational collapse,” *Phys. Rev.* **136** (1964) B571–B576, doi:10.1103/PhysRev.136.B571.

[11] Z.C. Li and H. Lü, “Regular electric black holes from Einstein-Maxwell-scalar gravity,” *Phys. Rev. D* **110**, no.10, 104046 (2024) doi:10.1103/PhysRevD.110.104046 [arXiv:2407.07952 [gr-qc]].

[12] F. Shojai, A. Sadeghi and R. Hassannejad, “Generalized Oppenheimer-Snyder gravitational collapse into regular black holes,” *Class. Quantum Grav.* **39** (2022) 085003, doi:10.1088/1361-6382/ac5924, [arXiv:2202.14024 [gr-qc]].

[13] E. Poisson and W. Israel, “Internal structure of black holes,” *Phys. Rev. D* **41** (1990) 1796–1809, doi:10.1103/PhysRevD.41.1796.

[14] Z.C. Li and H. Lü, “Regular black holes from analytic $f(F^2)$,” *Eur. Phys. J. C* **83** (2023) no.8, 755 doi:10.1140/epjc/s10052-023-11908-x [arXiv:2303.16924 [gr-qc]].

[15] M. Born and L. Infeld, “Foundations of the new field theory,” *Proc. Roy. Soc. Lond. A* **144** (1934) 425–451, doi:10.1098/rspa.1934.0059.

[16] T.K. Dey, “Born-Infeld black holes in the presence of a cosmological constant,” *Phys. Lett. B* **595** (2004) 484–490, doi:10.1016/j.physletb.2004.06.047, [arXiv:hep-th/0406169 [hep-th]].

[17] H.S. Liu, Z.F. Mai, Y.Z. Li and H. Lü, “Quasi-topological electromagnetism: dark energy, dyonic black holes, stable photon spheres and hidden electromagnetic duality,” *Sci. China Phys. Mech. Astron.* **63**, 240411 (2020) doi:10.1007/s11433-019-1446-1 [arXiv:1907.10876 [hep-th]].

[18] E. Ayón-Beato and A. García, “Regular black hole in general relativity coupled to nonlinear electrodynamics,” *Phys. Rev. Lett.* **80** (1998) 5056–5059, doi:10.1103/PhysRevLett.80.5056, [arXiv:gr-qc/9911046 [gr-qc]].

[19] E. Ayón-Beato and A. García, “New regular black hole solution from nonlinear electrodynamics,” *Phys. Lett. B* **464** (1999) 25–29, doi:10.1016/S0370-2693(99)01038-2, [arXiv:hep-th/9911174 [hep-th]].

[20] Z.Y. Fan and X. Wang, “Construction of regular black holes in general relativity,” *Phys. Rev. D* **94**, no.12, 124027 (2016) doi:10.1103/PhysRevD.94.124027 [arXiv:1610.02636 [gr-qc]].

[21] P. Bueno, P.A. Cano and R.A. Hennigar, “Regular black holes from pure gravity,” Phys. Lett. B **861** (2025), 139260 doi:10.1016/j.physletb.2025.139260 [arXiv:2403.04827 [gr-qc]].